Polarization of Molecular X-Ray Fluorescence

D. W. Lindle, P. L. Cowan, R. E. LaVilla, T. Jach, and R. D. Deslattes
National Bureau of Standards, Gaithersburg, Maryland 20899

B. Karlin
National Synchrotron Light Source, Brookhaven National Laboratory, Upton, New York 11973

and

J. A. Sheehy, T. J. Gil, and P. W. Langhoff
Department of Chemistry, Indiana University, Bloomington, Indiana 47405
(Received 7 December 1987)

Polarization of Cl $K\beta$ x-ray fluorescence following selective excitation of gaseous CH_3Cl with synchrotron radiation is reported. The degree of polarization of the fluorescence depends sensitively on the chosen incident excitation energy in the Cl K-edge region. Theoretical considerations indicate that the fluorescence-polarization measurements can provide directly absorption and emission anisotropies, molecular-orbital symmetries, and relative fluorescence transition strengths.

PACS numbers: 33.20.Rm, 33.50.Dq, 33.90.+h

X-ray emission spectroscopy under conditions of unpolarized excitation and detection has a long history of elucidating core-level phenomena in a wide variety of contexts.[1] Synchrotron-radiation sources in the x-ray range now provide both tunable and polarized exciting radiation throughout the spectral regions near core-level thresholds in atoms, molecules, and solids.[2] Combining the advantages offered by synchrotron radiation with polarization analysis of the x-ray fluorescence, we report here results of valence-electron x-ray fluorescence-polarization measurements following energy-selected and polarized excitation near the Cl K edge of methyl chloride (CH_3Cl). Theoretical interpretation of the measured polarized-fluorescence spectra indicates that the anisotropy of the photoexcitation process *and* the orientations and relative magnitudes of fluorescent dipole transition moments may be obtained directly from experiment. The x-ray polarized-fluorescence technique reported here thus provides a new approach to molecular photoabsorption and emission, as well as molecular-structure studies.

Previous work has used ultraviolet and visible fluorescence polarization to infer alignment of molecular ions and fragments following polarized excitation of *valence* electrons.[3] The present study reports initial observations of fluorescence polarization following *core*-level excitation.[4] For molecular systems, core-level studies offer two distinct advantages. First, because core levels undergo rapid Auger decay ($\leq 10^{-14}$ s), fluorescence is observed on a time scale that is short compared with normal molecular tumbling periods (10^{-11}-10^{-12} s). Valence-shell hole states, in contrast, are sufficiently long lived ($\geq 10^{-10}$ s) that rotational motion can occur prior to radiative decay, complicating the interpretation of fluorescence-polarization measurements.[3] Second, core-level spectroscopy is highly selective to a specific atomic absorption edge and, with sufficient resolution, to the same atomic species in different environments.

Core-level fluorescence-polarization measurements require (i) a source of polarized x rays, (ii) high-throughput and high-resolution primary *and* secondary x-ray monochromators, and (iii) polarization sensitivity of the secondary spectrometer. The first requirement is satisfied by synchrotron radiation, which in this work was provided by beam line X-24A at the National Synchrotron Light Source (NSLS), where a large-aperture crystal-diffraction primary monochromator selects the desired incident x-ray energy with a bandwidth of 0.4 eV.[5] The use of Si(111) crystals near the Cl K edge in the primary monochromator enhances the inherent linear polarization of the synchrotron radiation. The polarized monochromatic synchrotron radiation is focused into a gas cell containing 300-Torr CH_3Cl at room temperature. Ionization chambers are used to measure incident and transmitted flux in order to determine relative absorption as a function of photon energy.

An efficient secondary spectrometer detects the x-ray fluorescence emitted from the gas cell vertically upward at 90° with respect to the propagation direction of the synchrotron-radiation beam, with the incident polarization vector in the horizontal plane. The emitted x rays are energy analyzed ($\Delta E \simeq 0.9$ eV) in a curved-crystal secondary spectrometer by a position-sensitive detector so that a complete $K\beta$ spectrum is obtained. Polarization sensitivity of the secondary spectrometer is accomplished for Cl K-edge fluorescence (≈ 2.8 keV) by the use of a Si(111) crystal at a Bragg angle of 44.6°, providing strong rejection (10^3:1) of fluorescence polarized

out of the plane of the crystal surface. Polarization-specific fluorescence spectroscopy is then achieved by the placement of the dispersion plane of the secondary spectrometer either parallel or perpendicular to the synchrotron-radiation propagation direction, ensuring that only fluorescence polarized parallel or perpendicular, respectively, to the incident polarization is detected from the sample.

Figure 1 shows the measured absorption spectrum of CH_3Cl in the vicinity of the Cl K edge, as well as a Cl $K\beta$ fluorescence spectrum taken with an incident photon energy of 2880 eV, well above the Cl $1s$ threshold at 2828.5 eV.[6,7] The $K\beta$ spectrum at this incident energy is found to be independent of the fluorescence polarization within our experimental uncertainty. The pre-edge feature D in the absorption spectrum, of primary interest here, is attributed to a Cl $1s$ (CH_3Cl $1a_1$) excitation to the $8a_1$ antibonding molecular orbital. Figure 2 shows measured Cl $K\beta$ polarized-fluorescence spectra of CH_3Cl with an excitation energy of 2823.4 eV, centered on feature D of Fig. 1, taken in parallel and perpendicular polarizations. The relative intensities of the larger $K\beta$ peak C have been scaled equally in each spectrum for ease of comparison. The significant difference between the B-to-C peak ratios in the two polarizations of Fig. 2 is the essential new observation of this work.

In Figs. 1 and 2, the Cl $K\beta$ fluorescence peaks B and C result from the filling of a Cl $1s$ hole by electrons in valence molecular orbitals containing significant Cl $3p$ character. The relevant valence orbitals of CH_3Cl are $3e$, $7a_1$, and $2e$, with experimental binding energies of 11.3, 14.4, and 15.4 eV, yielding Cl $K\beta$ energies of 2817.1, 2814.0, and 2813.0 eV, respectively.[6,7] We observe just two peaks in the $K\beta$ spectra of Figs. 1 and 2 because the fluorescence due to the $2e$ and $7a_1$ orbitals is unresolved.

In Fig. 3 are shown the spatial characteristics, as well as calculated energies and f numbers, of the molecular orbitals of CH_3Cl that participate in the excitation and fluorescence processes associated with features B–D in Figs. 1 and 2. If we neglect for the moment the weaker $2e \rightarrow 1a_1$ contribution to peak B, Fig. 3 provides a qualitative clarification of the experimental data. Specifically, molecules excited with incident energies on absorption feature D ($1a_1 \rightarrow 8a_1$) have their symmetry axes oriented largely in the synchrotron-radiation polarization direction. The subsequent $K\beta$ radiative decay reflects the molecular alignment produced by the excitation. Consequently, fluorescence peak B ($7a_1 \rightarrow 1a_1$) should be stronger relative to fluorescence peak C ($3e \rightarrow 1a_1$) when observed in parallel rather than in perpendicular polarization, because the $7a_1 \rightarrow 1a_1$ transition also is polarized along the symmetry axis. When the excitation energy is 2880 eV, well above threshold, the absorption process is expected to be more isotropic than at 2823.4 eV (on feature D), so that the polarization effect on the B-to-C fluorescence intensity ratio should diminish, in accordance with observation (Fig. 1).

Quantitative interpretation of the data of Figs. 1 and 2 is based on the classical treatment of fluorescence polarization due to Jablonski[8] and others,[9-11] and molecular-orbital and static-exchange calculations of the occupied and virtual states.[12] The fluorescence-line polarization P

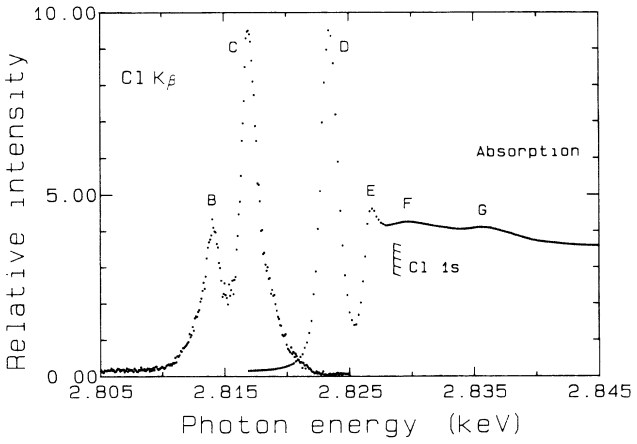

FIG. 1. Cl K-edge absorption spectrum (right) and Cl $K\beta$ emission spectrum (left) of CH_3Cl. The $K\beta$ spectrum was taken with 0.9-eV resolution at an excitation energy of 2880 eV, and exhibits no detectable change with fluorescence polarization. Peak labels and the Cl $1s$ ($1a_1$ in CH_3Cl) threshold energy are adopted from Refs. 6 and 7.

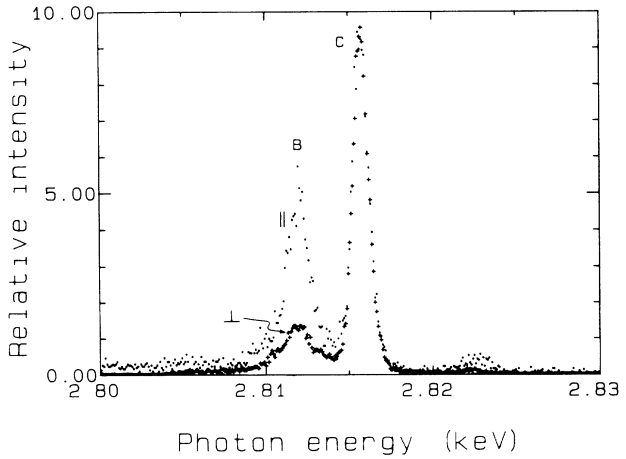

FIG. 2. Cl $K\beta$ fluorescence spectra from CH_3Cl following Cl $1s \rightarrow 8a_1$ excitation with 2823.4-eV photon energy, centered on feature D in the absorption spectrum of Fig. 1. The labels parallel and perpendicular refer to orthogonal orientations of the measured fluorescence polarization relative to the incident E vector. The two spectra have been scaled so that the areas of peak C are identical. The peak at 2823.4 eV is due to elastic scattering of the incident radiation.

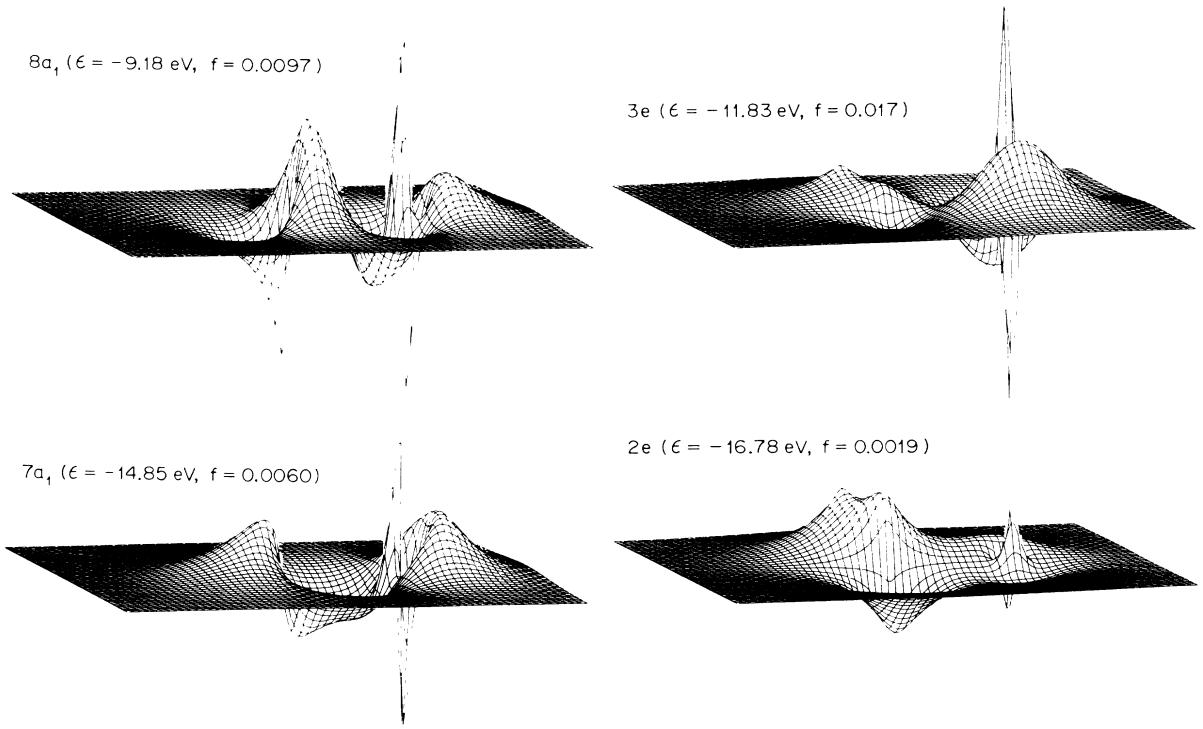

FIG. 3. Occupied and virtual molecular orbitals of CH_3Cl participating in the excitation and fluorescence decay processes giving rise to the measured spectra of Figs. 1 and 2. The drawings refer to molecular-orbital amplitudes in a plane containing the Cl and C atoms, as well as one H atom, with Cl on the right and the methyl group on the left. Orbital energies in electronvolts and f numbers with the Cl 1s orbital are given also.

in the present geometry takes the form[8-10]

$$P=\frac{I_{\parallel}-I_{\perp}}{I_{\parallel}+I_{\perp}}=\frac{a_{\parallel}f_{\parallel}-a_{\parallel}f_{\perp}-a_{\perp}f_{\parallel}+a_{\perp}f_{\perp}}{2a_{\parallel}f_{\parallel}+3a_{\parallel}f_{\perp}+3a_{\perp}f_{\parallel}+7a_{\perp}f_{\perp}}, \quad (1)$$

where $I_{\parallel}$ and $I_{\perp}$ refer to integrated intensities of fluorescence peaks in parallel or perpendicular polarization, respectively. In the last expression in Eq. (1), which is applicable for randomly oriented molecules frozen in space,[8-10] $a_{\parallel}$ and $a_{\perp}$ are the body-frame absorption intensities (dipole transition moments or f numbers) for incident polarization parallel and perpendicular, respectively, to the molecular symmetry axis. The $f_{\parallel}$ and $f_{\perp}$ are the corresponding quantities in emission, which can be different for each of the three fluorescence transitions, as indicated in Fig. 3. In fact, for CH_3Cl, $f_{\parallel}=0$ for the transitions $2e\rightarrow 1a_1$ and $3e\rightarrow 1a_1$, and $f_{\perp}=0$ for the transition $7a_1\rightarrow 1a_1$.

For 2880-eV excitation, the equality of observed fluorescence profiles in orthogonal polarizations (Fig. 1) indicates that the values of P for peaks B and C are equal within experimental error. Exact equality of P values is possible only if P is zero for both peaks, in which case $a_{\parallel}$ and $a_{\perp}$ are identical at 2880 eV [see Eq. (1)]. Unfortunately, a definitive statement on this latter point is precluded by experimental uncertainty, because of an insensitivity of P to the measured intensity ratios. Nevertheless, the measured B-to-C peak intensity ratio in either polarization and for excitation well above threshold can yield directly the ratio

$$[f_{\parallel}(7a_1\rightarrow 1a_1)+f_{\perp}(2e\rightarrow 1a_1)]/f_{\perp}(3e\rightarrow 1a_1).$$

The measured (Fig. 1) and calculated (Fig. 3) ratios are 0.54(5) and 0.46, respectively.

In the case of peak-D excitation (Fig. 2), $a_{\perp}=0$ in Eq. (1) so that $P=-\frac{1}{3}$ for the transitions $2e\rightarrow 1a_1$ and $3e\rightarrow 1a_1$, and $P=\frac{1}{2}$ for the transition $7a_1\rightarrow 1a_1$. If we employ these polarization values and the spectral assignments, two expressions for the B-to-C peak ratios in the orthogonal polarization spectra of Fig. 2 are obtained in the forms[13]

$$\frac{I_{B\parallel}}{I_{c\parallel}}=\frac{\frac{9}{4}f_{\parallel}(7a_1\rightarrow 1a_1)+f_{\perp}(2e\rightarrow 1a_1)}{f_{\perp}(3e\rightarrow 1a_1)}, \quad (2a)$$

$$\frac{I_{B\perp}}{I_{c\perp}}=\frac{\frac{3}{8}f_{\parallel}(7a_1\rightarrow 1a_1)+f_{\perp}(2e\rightarrow 1a_1)}{f_{\perp}(3e\rightarrow 1a_1)}. \quad (2b)$$

The measured B-to-C intensity ratios are 0.86(5) and 0.29(2) for parallel and perpendicular polarizations (Fig. 2), respectively, whereas the corresponding calculated values are 0.90 and 0.24 (Fig. 3). The experimental

values inferred from the results in Fig. 2 for the relative f numbers

$$[f_{\parallel}(7a_1 \rightarrow 1a_1)/f_{\perp}(3e \rightarrow 1a_1) = 0.30(3),$$

$$f_{\perp}(2e \rightarrow 1a_1)/f_{\perp}(3e \rightarrow 1a_1) = 0.18(2)]$$

also compare favorably with the calculated values [0.35;0.11]. Moreover, the fluorescence spectra of Figs. 1 and 2 are in reasonable quantitative accord in that the sum [0.48(5)] of the two relative f numbers inferred from Eqs. (2) agrees with that [0.54(5)] obtained directly from the $K\beta$ spectrum in Fig. 1. Additional experimental and theoretical results, including absolute fluorescence-polarization values P in Ch_3Cl and other compounds as a function of excitation energy, will be reported separately.

In summary, we have observed significant polarization of x-ray fluorescence following resonant excitation of CH_3Cl near the Cl K edge. This effect is a consequence of the alignment of the molecule produced by the excitation process. Theoretical considerations provide a direct and sensible interpretation of the measurements, with the calculated relative transition strengths and inferred orbital symmetries in good accord with those derived directly from experiment. We expect the x-ray polarized-fluorescence phenomenon to aid in the assignment of resonant features in the core-level absorption spectra of a wide variety of species in many environments, including adsorbate and condensed phases.

The experiments were performed at the National Synchrotron Light Source, which is supported by the U.S. Department of Energy under Contract No. AC020-76CH00016. Three of us (J.A.S., T.J.G., and P.W.L.) also acknowledge support by the National Science Foundation under Grant No. CHE86-14344. Computational support provided by the National Center for Supercomputing Applications is gratefully acknowledged.

[1]A. Meisel, G. Leonhardt, and R. Szargan, *Röntgenspectren und chemische Bindung* (Akademische Verlagsgesellschaft, Leipzig, 1977).

[2]R. D. Deslattes, R. E. LaVilla, P. L. Cowan, and A. Henins, Phys. Rev. A **27**, 923 (1983); R. D. Deslattes, Aust. J. Phys. **39**, 845 (1986).

[3]See, for example, E. D. Poliakoff, J. L. Dehmer, D. Dill, A. C. Parr, K. H. Jackson, and R. N. Zare, Phys. Rev. Lett. **46**, 907 (1981); E. D. Poliakoff, J. L. Dehmer, A. C. Parr, and G. E. Leroi, J. Chem. Phys. **77**, 5243 (1982); J. W. Keller, W. T. Hill, III, D. L. Ederer, T. J. Gil, and P. W. Langhoff, J. Chem. Phys. **87**, 3299 (1987).

[4]Some previous observations of core-level fluorescence polarization from single crystals have been reported, but with unpolarized, fixed-energy excitation rendering them insensitive to near-threshold spectral features. See, for example, G. Dräger and O. Brümmer, in Proceedings of the International Conference on X-Ray and Inner-Shell Processes in Atoms, Molecules, and Solids (X84), Leipzig, East Germany, 1984, edited by A. Meisel and J. Finster (to be published).

[5]P. L. Cowan, S. Brennan, R. D. Deslattes, A. Henins, T. Jach, and E. G. Kessler, Nucl. Instrum. Methods Phys. Res. Sect. A **246**, 154 (1986).

[6]R. D. Deslattes and R. E. LaVilla, Appl. Opt. **6**, 39 (1967).

[7]R. C. C. Perera, J. Barth, R. E. LaVilla, R. D. Deslattes, and A. Henins, Phys. Rev. A **32**, 1489 (1985).

[8]A. Jablonski, Z. Phys. **96**, 236 (1935).

[9]P. P. Feofilov, *The Physical Basis of Polarized Emission* (Consultants Bureau, New York, 1961).

[10]B. I. Stepanov and V. P. Gribkovskii, *Theory of Luminescence* (Iliffe, London, 1968).

[11]C. H. Greene and R. N. Zare, Annu. Rev. Phys. Chem. **33**, 119 (1982).

[12]P. W. Langhoff, in *Methods in Computational Molecular Physics,* edited by S. Wilson and G. H. F. Diercksen (Reidel, Dordrecht, 1983).

[13]The polarization values $P = -\frac{1}{3}$ and $P = \frac{1}{2}$ imply $I_{\perp}/I_{\parallel} = 2$ and $I_{\perp}/I_{\parallel} = \frac{1}{3}$, respectively, with use of Eq. (1). Because of $I_{\parallel} + I_{\perp} \propto f$, we have $I_{\parallel} \propto \frac{3}{4} f$ and $I_{\perp} \propto \frac{1}{4} f$ for the transition $7a_1 \rightarrow 1a_1$. Similarly, we find $I_{\parallel} \propto \frac{1}{3} f_{\perp}$ and $I_{\perp} \propto \frac{2}{3} f_{\perp}$ for the transitions $3e \rightarrow 1a_1$ and $2e \rightarrow 1a_1$. Equations (2a) and (2b) then follow directly, with use of the spectral assignments discussed in the text.

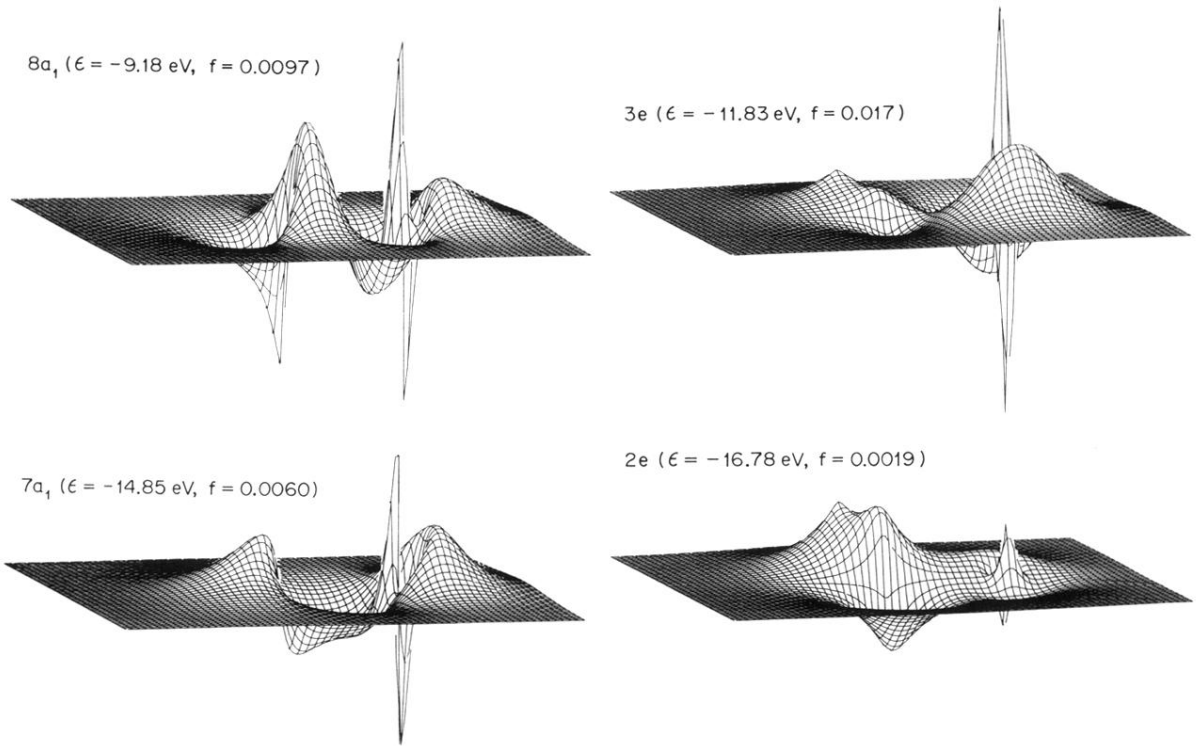

FIG. 3. Occupied and virtual molecular orbitals of CH_3Cl participating in the excitation and fluorescence decay processes giving rise to the measured spectra of Figs. 1 and 2. The drawings refer to molecular-orbital amplitudes in a plane containing the Cl and C atoms, as well as one H atom, with Cl on the right and the methyl group on the left. Orbital energies in electronvolts and f numbers with the Cl 1s orbital are given also.